Available online at www.sciencedirect.com
ScienceDirect
Journal of Magnetic Resonance 187 (2007) 258–265
JMR Journal of Magnetic Resonance
www.elsevier.com/locate/jmr

Compensated adiabatic inversion pulses: Broadband INEPT and HSQC

Eriks Kupče, Ray Freeman *

Varian, Ltd, 6 Mead Road, Yarnton, Oxford, UK
Jesus College, Cambridge University, Cambridge CB5 8BL, UK

Received 6 March 2007; revised 3 May 2007
Available online 17 May 2007

Abstract

When adiabatic fast passage is used to flip nuclear spins, sites with different chemical shifts are inverted at different times, causing refocusing errors. By mapping the phase evolution diagrams, we show that these effects can be accurately compensated with matched pairs of adiabatic pulses, either opposed or in the same sense, depending on the application. Applied to well-known heteronuclear polarization transfer experiments such as INEPT and HSQC, the requisite evolution of *J*-vectors is achieved irrespective of chemical shift or the duration of the adiabatic sweeps. By replacing conventional 180° pulses, these new adiabatic sequences offer an order of magnitude improvement in effective bandwidth for the X-spins. Alternatively the experiments can be carried out with significantly reduced radiofrequency power. One- and two-dimensional spectra of ^{13}C in 13-*cis*-retinal at 600 MHz have been used to demonstrate these advantages.

Keywords: Adiabatic pulses; Broadband inversion; HSQC; INEPT; Retinal; SCARPER

1. Introduction

An essential feature of many pulse sequences employed in high-resolution NMR spectroscopy is the spin inversion element, often implemented as a hard 180° radiofrequency pulse. For nuclei with a wide range of chemical shifts, and particularly at high magnetic fields, the effective bandwidth of such pulses may prove inadequate. Composite 180° pulses [1–3] may alleviate the problem to some extent, as in certain broadband decoupling schemes [4–8] but the quest for wider and wider bandwidths continues. Adiabatic pulses appear to offer the best solution, as demonstrated by the impressive improvements that have been achieved in broadband heteronuclear decoupling [9–17]. The goal is to cover a much wider X-spin bandwidth with relatively low radiofrequency power. In addition, adiabatic fast passage has a further advantage. Provided that the adiabatic condition [18] is satisfied, the inversion efficiency is independent of the intensity of the radiofrequency field. This means that careful calibration is no longer required, and that the inversion efficiency is insensitive to any spatial inhomogeneity of the radiofrequency field.

It is not simply a question of replacing each 180° pulse with the equivalent adiabatic inversion pulse. The problem is that an adiabatic sweep has an appreciable duration, of the order of a millisecond. As the frequency is swept, there are significant variations in the time at which inversion occurs for spins with different chemical shifts. This is known to complicate any experiment that relies on refocusing (or on acquiring a prescribed divergence) of scalar coupling vectors.

Several groups have addressed this problem [19–27]. One approach exploits the roughly linear relationship between single-bond ^{13}CH coupling constants and ^{13}C chemical shifts, so that by judicious choice of the adiabatic sweep rate and direction, an approximate focus can be achieved [25,26]. Another solution [27] is to employ a composite sequence of three adiabatic pulses where the central pulse flips the effective radiofrequency field, allowing the third pulse to reverse the phase errors of the first. In the present article we use a method related to the concept of the ''double-echo'' where the phase deviations of the first spin echo are compensated on the second echo [19,28,29].

* Corresponding author. Fax: +44 1223 336362.
E-mail address: rf110@hermes.cam.ac.uk (R. Freeman).

1090-7807/$ - see front matter © 2007 Elsevier Inc. All rights reserved.
doi:10.1016/j.jmr.2007.05.009

Adiabatic pulses are applied in matched pairs in such a manner that the variations in the inversion times are compensated by the second sweep [30]. We seek the most effective implementations of this idea in the standard heteronuclear polarization transfer schemes, INEPT [31] and HSQC [32,33].

2. Phase evolution diagrams

2.1. Evolution of the proton spins

Consider the case of a pulse sequence designed to generate an antiphase alignment of magnetization vectors due to spin coupling evolution, as in the preparation stage of the INEPT experiment. For this case, proton spins are the ones being manipulated prior to polarization transfer to another nuclear species, X. The critical stage involves the inversion of the X-spins over a wide range of chemical shifts. It has been demonstrated [30] that the requisite compensation can be achieved by using a pair of adiabatic pulses with opposite senses of frequency sweep. In all other respects (duration, sweep rate, radiofrequency level) the two adiabatic pulses are exactly matched.

Fig. 1 illustrates this mode of compensation by mapping the phase evolution of two spin packets (labelled red and blue) representing two arbitrary X-spin chemical shifts. The key feature [30] is the reversal of the sweep direction of the second adiabatic pulse; this is represented in Fig. 1 by reversing the order of the red and blue spin packets. Because the first sweep inverts the blue spins later than the red spins, this time lag is compensated as the second sweep inverts the blue spins *before* the red spins. Consequently both phase evolution trajectories come back into coincidence at the end of the sequence. Consider a site with coupling constant J_{XH} that experiences an arbitrary delay d after the start of the adiabatic sweep. The scalar coupling vectors accumulate final phase angles ϕ that are independent of all time lags d and the choice of adiabatic sweep duration T.

$$\begin{aligned}\phi &= \pm 0.5 J_{XH}[d - T + d + \delta - d + T - d + \delta] \\ &= \pm J_{XH}\delta \end{aligned} \quad (1)$$

With the usual condition $J_{XH}\delta = \pi/2$, the required antiphase alignment is achieved. Naturally if the chemical sites involved have different heteronuclear coupling constants, there are deviations from this optimum condition.

2.2. Evolution of the X-spins

Consider the phase evolution diagram for the case where antiphase magnetization has already been transferred to a heteronuclear species X, as at the end of an INEPT stage. It is convenient to treat here the equivalent general case where the X-spins are excited with the two J-vectors initially in phase, and evolve into the antiphase configuration at the end of the sequence (Fig. 2). In both cases the requirements are that the chemical shift evolution be refocused and that the J-vectors evolve through $\pm\pi/2$. The chemical shift effect can be compensated by a pair of adiabatic pulses with the *same* sense of frequency sweep. For an arbitrary chemical shift ν and an arbitrary time lag d, the net phase evolution of the X-spin due to its chemical shift is given by:

$$\phi = \nu[d - T + d - \Delta - d + T - d + \Delta] = 0 \quad (2)$$

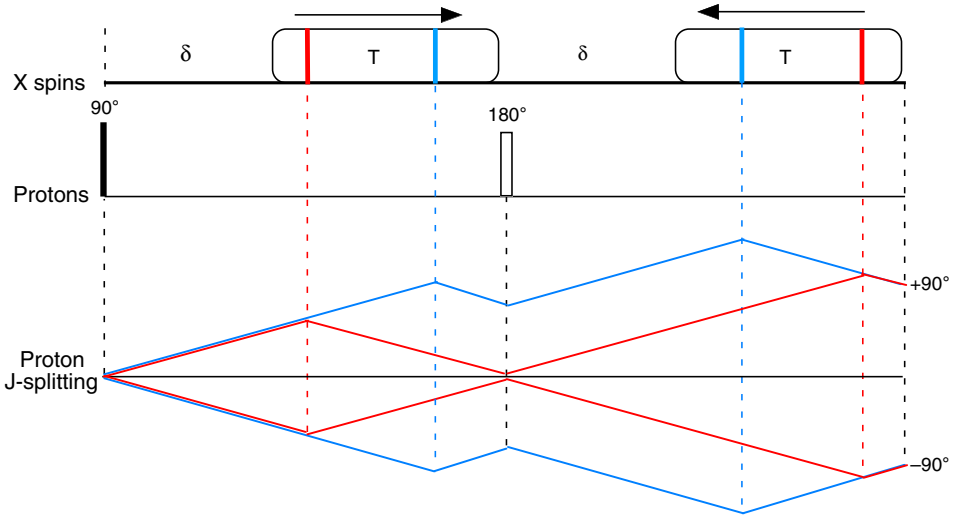

Fig. 1. Phase evolution diagram showing compensation for variations in the instant of adiabatic spin inversion due to different X-spin chemical shifts. The proton chemical shifts are refocused and the proton J-vectors evolve into the antiphase configuration. The intervals δ and T are of comparable lengths (ms). The key feature is the reversal of the sweep direction of the second adiabatic pulse (shown symbolically by the reversed arrow). The trajectories of the red and blue spin packets (representing arbitrary X-spin chemical shifts) converge at the end of the sequence to give the desired antiphase configuration. The same result is obtained if both δ and T intervals are interchanged. (For interpretation of the references to colour in this figure legend, the reader is referred to the web version of this article.)

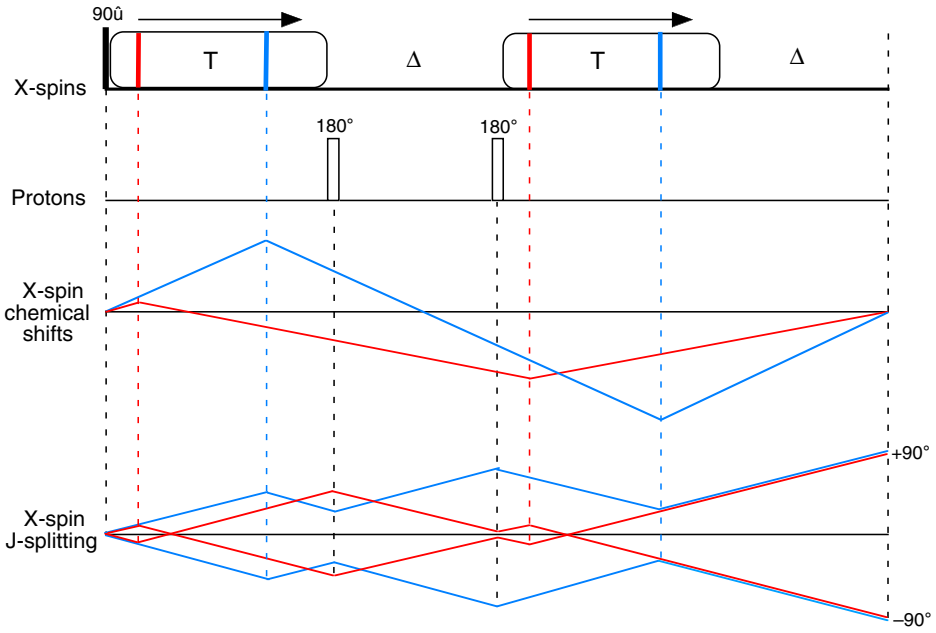

Fig. 2. Phase evolution diagram showing compensation for variations in the instant of adiabatic spin inversion due to different X-spin chemical shifts. The X-spin chemical shifts are refocused, and the X-spin J-vectors evolve into the antiphase configuration. In contrast to Fig. 1, the two adiabatic sweeps are now in the same direction. Red and blue vectors represent arbitrary chemical shifts of the X-spins. The key feature is the reversal of the sense of J-evolution during the first Δ interval, achieved by the pair of 180° pulses applied to the protons. The same result is obtained if both Δ and T intervals are interchanged. (For interpretation of the references to colour in this figure legend, the reader is referred to the web version of this article.)

That is to say that all chemical shift effects are refocused, irrespective of the choice of Δ and T. At first sight such an arrangement would seem to preclude refocusing of the J-vectors. However, the phase evolution diagram of Fig. 2 demonstrates that the introduction of a pair of 180° proton pulses flanking the first Δ interval temporarily reverses the sense of the J-evolution, thus generating the desired phase divergence:

$$\phi = \pm 0.5 J_{XH}[d - T + d + \Delta - d + T - d + \Delta] = \pm J_{XH}\Delta \tag{3}$$

By an analogous argument, an initial antiphase condition would be converted into exact alignment at the end of the sequence.

The analyses of both these manipulations neglect the very short time required to invert the spins at a given site. During the actual inversion, the two J-vectors can be thought of as being temporarily spin-locked along the strong effective radiofrequency field, thereby suspending J-evolution. However, this tiny correction cancels, because it slightly shortens the effective durations of both adiabatic pulses equally, and the final phase accumulations are independent of these durations, provided they are equal.

3. Applications

3.1. Compensated broadband INEPT

One of several possible applications of these compensation schemes is the INEPT [31] building block, widely used in many standard NMR pulse sequences. The preparation stage, designed to create an antiphase alignment of proton vectors, employs the sequence of Fig. 1 with the pair of adiabatic pulses sweeping in opposite directions [30]. A 90° proton pulse (about the Y-axis) generates longitudinal two-spin order ($2I_ZS_Z$), converted into antiphase X-spin magnetization by the X-spin pulse of flip angle α. The next stage follows the equivalent of the sequence in Fig. 2 (with both adiabatic sweeps in the *same* direction), refocusing the X-spin chemical shifts and bringing the J-vectors back into alignment (Fig. 3). All the variations in the instant of spin inversion are compensated. A final 90° pulse on the protons removes any remaining antiphase magnetization; thereby minimizing the amplitude of the residual decoupling sidebands.

Whereas conventional INEPT uses hard 180° pulses for spin inversion, the adiabatic pulse modification achieves much wider effective bandwidths, as can be appreciated from Fig. 4 which compares the frequency profiles of the conventional and wideband versions of INEPT for ^{13}C spectra from an enriched methyl iodide sample. WURST-40 adiabatic pulses [13,15] were employed with a peak radiofrequency level (expressed in frequency units) of 5.5 kHz. In these tests the adiabatic sweep duration ($T = 2$ ms) was deliberately set above its usual value to make it comparable with the evolution period, in order to emphasize the compensation effect. Shorter sweep durations could be used in practice (but at the expense of increased radiofrequency power dissipation).

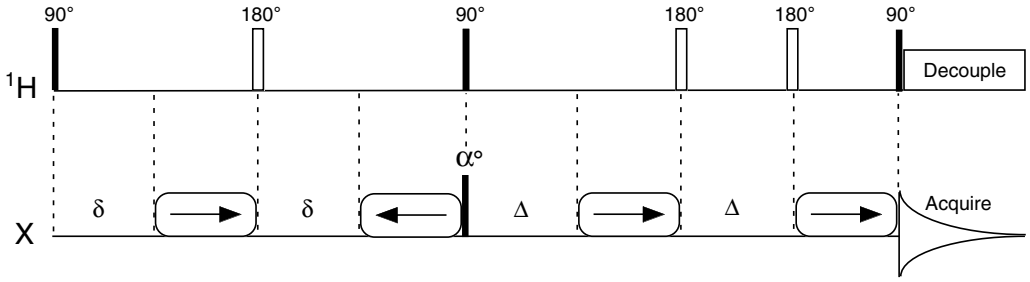

Fig. 3. Pulse sequence used for broadband INEPT, compensated for the variations in the instant of adiabatic spin inversion of different X-spin chemical sites. Note the reversed sweep direction of the second adiabatic pulse. The WURST-40 adiabatic pulses were implemented with the standard Varian software (P-box). They were phase-incremented in 1 μs steps up to a pulse duration of 2 ms.

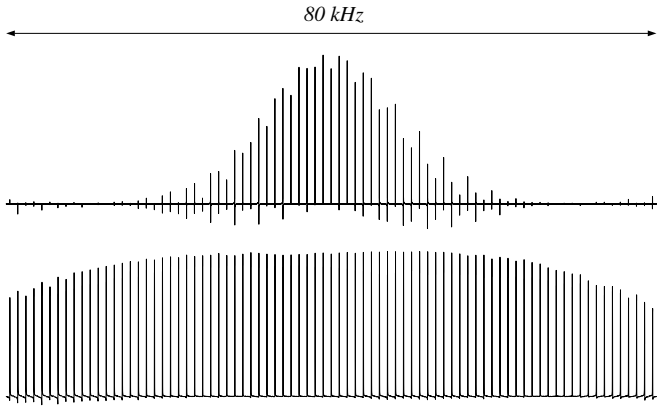

Fig. 4. Frequency profile for ^{13}C INEPT signals from an enriched methyl iodide sample using the conventional hard 180° inversion pulse (upper trace) compared with the profile when matched pairs of adiabatic pulses are employed (lower trace).

The spin inversion profile recorded with matched adiabatic pulses spans almost 80 kHz, an order of magnitude wider than the conventional mode. The latter suffers the additional disadvantage of phase and intensity anomalies, attributed to off-resonance rotations. The method has been further tested on the ^{13}C INEPT spectra of a 2.5% solution of 13-*cis*-retinal (Scheme 1) in $CDCl_3$ where the adiabatic sweep version enjoys more uniform intensities and is free from the phase anomalies evident when conventional 180° pulses are employed (Fig. 5).

3.2. Broadband-enhanced HSQC

There are some widely used NMR pulse sequences, such as heteronuclear single-quantum correlation (HSQC) experiments [32], where broadband spin inversion of the X-spins would be a decided advantage. If this is to be implemented by matched pairs of adiabatic pulses, even more stringent compensation conditions become necessary—chemical shift and *J*-coupling effects must be refocused both for protons and for the X-spins. The incorporation of the compensation scheme set out in Fig. 2 achieves this goal. The full phase evolution diagram is set out in Fig. 6. The 90° pulse on the X-spins at time $2(\Delta + T)$ transfers the useful coherence to the protons, so from this point only proton chemical shifts and scalar coupling evolution need be considered. At the same instant, the 180° pulse applied to the protons refocuses the proton chemical shifts after a further interval of $2T$. Evolution of the proton *J*-vectors during the $2T$ interval is refocused by the matched pair of adiabatic pulses applied to the X-spins.

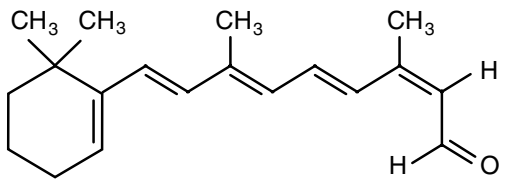

Scheme 1.

The new pulse sequence (Fig. 7) is based on the sensitivity-enhanced version [33] of the standard ^{13}C-HSQC experiment [32]. All X-spin inversions are achieved by matched pairs of adiabatic pulses. Typically $\delta = 1.6$ ms, $\lambda = 2.3$ ms, $\Delta = 1.8$ ms, $\zeta = 0.8$ ms. It is convenient to break down the full sequence into seven consecutive stages. The product operator formalism is used to describe the spin manipulations, with $S =$ protons, $I = {}^{13}$C. A ^{13}C pulse about the *Y*-axis of the rotating frame is written $[I_Y]$.

(1) Between points *A* and *B* the compensated INEPT sequence (Fig. 1) yields the term $+2I_YS_Z$.
(2) Between points *B* and *C*, chemical shift evolution of ^{13}C (with J_{IS} refocused by the 180° proton pulse) generates the terms:

$$+2I_YS_Z\cos(\omega_I t_1) - 2I_XS_Z\sin(\omega_I t_1).$$

(3) Between points *C* and *D*, the λ delays and the compensated pair of adiabatic pulses refocus the ^{13}C coherence-encoding gradients. Only ^{13}C chemical shifts are refocused in this interval.
(4) At point *D*, simultaneous 90° pulses $[S_X]$ and $[I_X]$ achieve the conversion:

$$+2I_YS_Z\cos(\omega_I t_1) - 2I_XS_Z\sin(\omega_I t_1)$$
$$\rightarrow -2I_ZS_Y\cos(\omega_I t_1) + 2I_XS_Y\sin(\omega_I t_1).$$

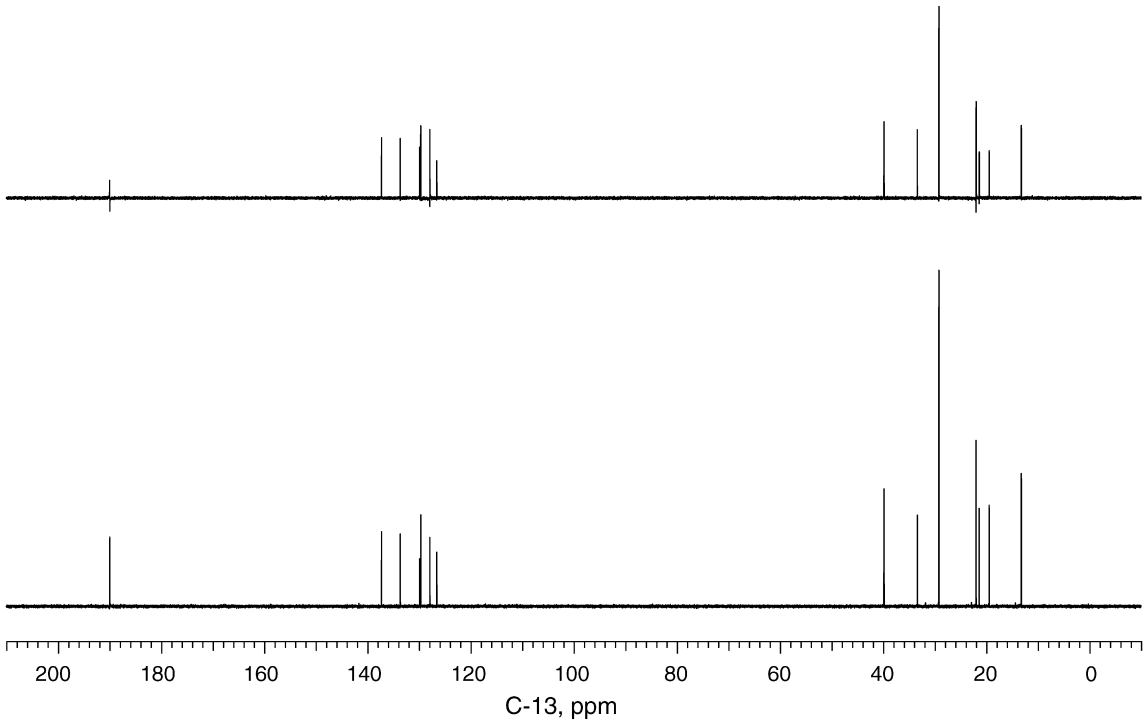

Fig. 5. Comparison of ^{13}C INEPT spectra of 13-*cis*-retinal recorded with the conventional hard 180° inversion pulse (upper trace) and with matched pairs of adiabatic inversion pulses (lower trace). Note the phase and intensity anomalies in the upper trace.

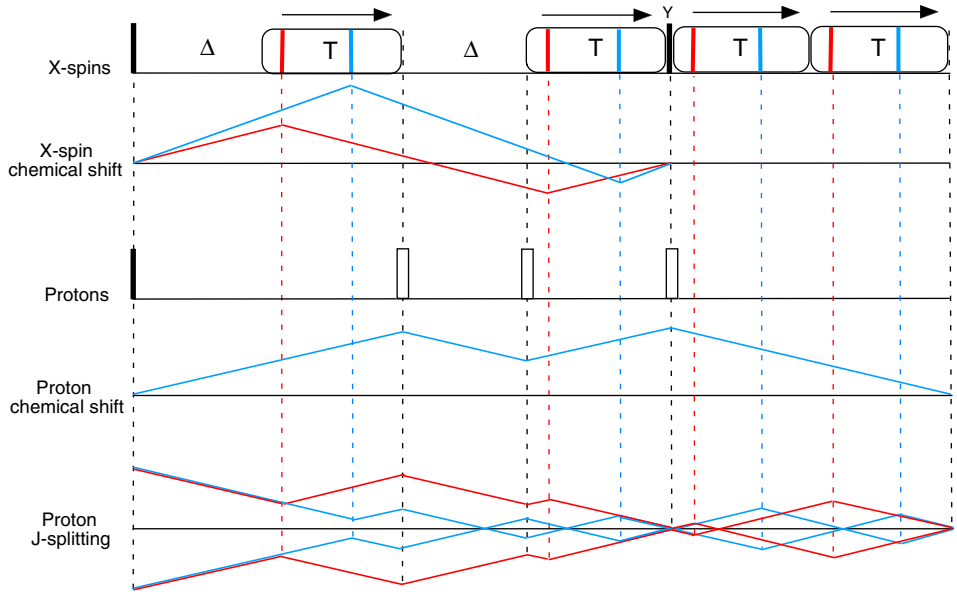

Fig. 6. Phase evolution diagram for the sequence that refocuses chemical shift evolution of both protons and X-spins. The X-spin chemical shifts come to a focus at time $2(T+\Delta)$ when the useful coherence is transferred to protons by the 90° (Y) pulse. At the end of the following interval $2T$, the proton chemical shifts come to a focus, and proton J-evolution is brought to a second focus by the matched pair of adiabatic pulses.

Between points D and E a version of the scheme shown in Fig. 6 is employed with compensated evolution of J-vectors, giving:

$$+S_X \cos(\omega_I t_1) + 2I_X S_Y \sin(\omega_I t_1).$$

At point E a ^{13}C pulse $[I_Y]$ and proton spin inversion $[S_X]$, $[S_X]$ create:

$$+S_X \cos(\omega_I t_1) + 2I_Z S_Y \sin(\omega_I t_1).$$

(5) Between points E and F the $2T$ interval allows the proton chemical shifts to reach a focus, while a matched pair of adiabatic pulses refocuses the scalar coupling evolution. Then at point F a proton pulse $[S_Y]$ generates:

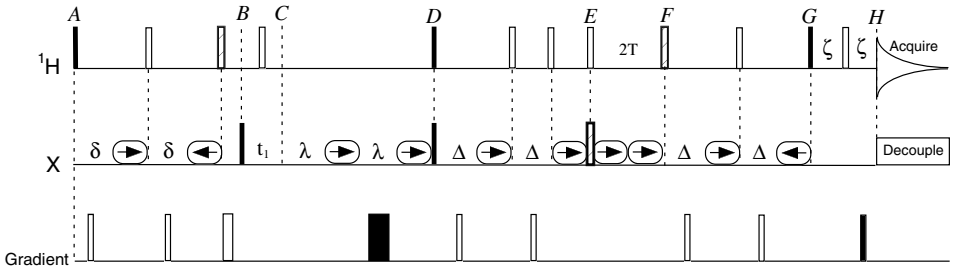

Fig. 7. Pulse sequence for the sensitivity-enhanced broadband HSQC experiments (see text for details). Black rectangles are 90° (X) radiofrequency pulses, hatched rectangles 90° (Y) pulses, open rectangles 180° pulses. The gradient pulses all have durations of 0.5 ms, except the third (1.0 ms) and fourth (2.0 ms). It is not feasible to represent relative gradient intensities accurately in this figure; they all have 2.5 G/cm, except for the third pulse (11 G/cm), fourth (24 G/cm) and last (24 G/cm). The black gradient pulses are used for coherence selection. Phase cycling (not shown) is the same as in Palmer et al. [33].

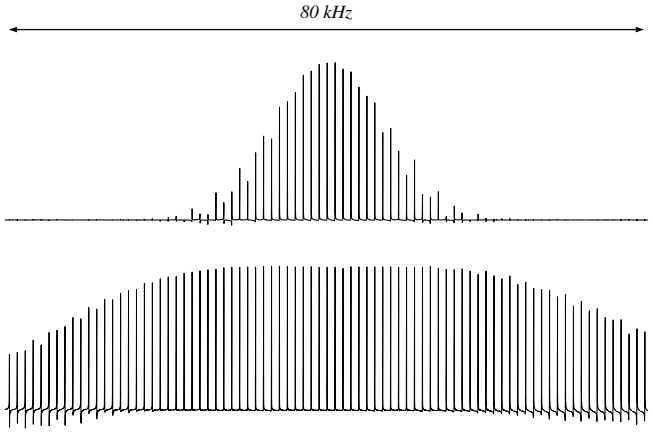

Fig. 8. Comparison of frequency profiles for sensitivity-enhanced ^{13}C HSQC signals of methyl iodide, using conventional hard 180° pulses (upper trace) and matched pairs of adiabatic inversion pulses (lower trace).

$$-S_Z\cos(\omega_I t_1) + 2I_Z S_Y \sin(\omega_I t_1).$$

(6) Between points F and G, compensated J-evolution takes place giving:

$$-S_Z\cos(\omega_I t_1) - S_X \sin(\omega_I t_1).$$

A final proton pulse [S_X] generates the orthogonal proton signals:

$$+S_Y\cos(\omega_I t_1) - S_X \sin(\omega_I t_1).$$

(7) The final interval between G and H serves simply to refocus the coherence-encoding gradients. The two orthogonal proton signals are then acquired in the normal manner with ^{13}C decoupling.

The increased ^{13}C bandwidth achieved by adiabatic pulses is demonstrated in Fig. 8, where frequency profiles are compared for HSQC spectra of methyl iodide using hard 180° pulses and adiabatic spin inversion. An order

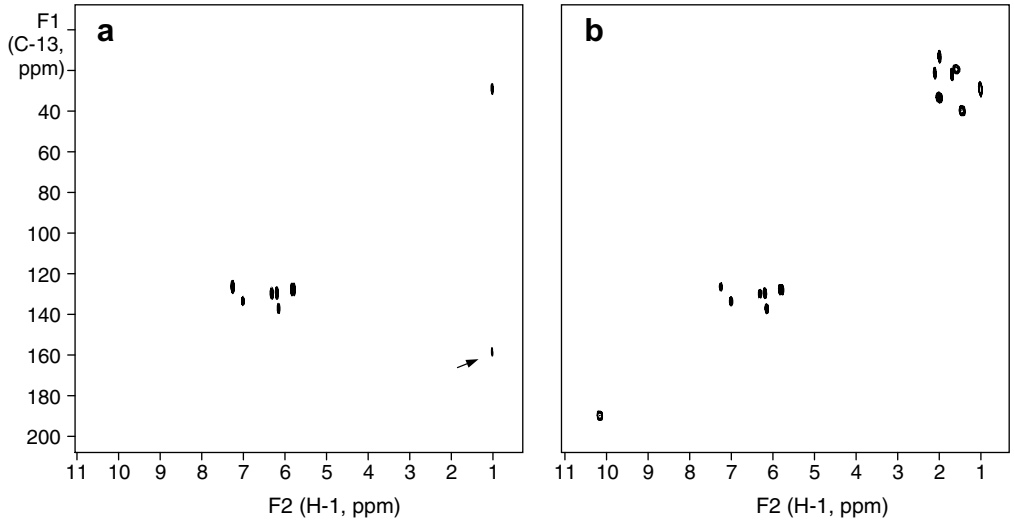

Fig. 9. (a) The sensitivity-enhanced ^{13}C HSQC spectrum of 13-*cis*-retinal recorded using conventional hard 180° inversion pulses. Note the artifact peak (arrowed) attributed to 180° pulse imperfections, and the loss of genuine signals due to the limited inversion bandwidth. (b) Corresponding spectrum obtained with matched pairs of adiabatic inversion pulses. To improve the clarity of presentation the correlation peaks in (a) and (b) have been artificially broadened by a factor of two in both frequency dimensions.

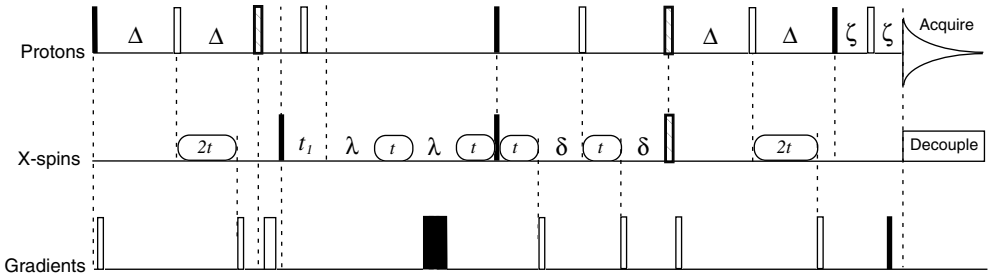

Fig. 10. A simplification of the compensated HSQC sequence that relies on the roughly linear relation between ^{13}C chemical shifts and ^{13}C–H scalar coupling constants. Black rectangles are 90° (X) pulses, hatched rectangles 90° (Y) pulses, open rectangles 180° pulses. The adiabatic sweeps are all in the same sense (from ^{13}C methyl towards aromatics) and have durations $t = 0.6$ ms or $2t = 1.2$ ms. If J_0 is the scalar ^{13}C–H coupling in the centre of the ^{13}C shift range, $\delta = 0.25/J_0$ and $\Delta = \delta + t$. The gradient pulses are as in Fig. 7. The intervals λ and ξ are equal to the gradient lengths plus the gradient recovery times. Phase cycling (not shown) is the same as in Palmer et al. [33].

of magnitude improvement is observed. Since the bandwidth of the adiabatic pulses can be made arbitrarily wide, the off-resonance performance of the sequence is limited essentially by the bandwidth of the 90° pulses. The predicted improvements are borne out by the comparison of ^{13}C HSQC spectra of 13-*cis*-retinal recorded on a Varian 600 MHz spectrometer and shown in Fig. 9. With conventional 180° pulses, several genuine responses are missing from the extrema of the ^{13}C chemical shift range, and there is a false response, indicated by the arrow, attributed to radiofrequency pulse imperfections.

When X is ^{13}C, it is possible to simplify the compensated HSQC sequence of Fig. 7 by exploiting the roughly linear relation between ^{13}C chemical shifts and ^{13}C–H coupling constants [25,26,30]. This modification is shown in Fig. 10. The adiabatic sweeps are all in the same direction (from ^{13}C methyls to aromatics) and have durations $t = 0.6$ ms or $2t = 1.2$ ms. The delays are determined by the value of J_0 (assumed to be 145 Hz) in the centre of the chemical shift range. Measurements on the retinal sample indicate that this sequence reliably reproduces the ^{13}C intensities in this case.

We call the new compensation technique SCARPER (self-compensating adiabatic rapid passage evolution regime). Scarper is British slang for "go quickly, run away" [34]; it is used here to emphasize the very high speed sweeps employed in these adiabatic experiments, typically 50 MHz s^{-1} for ^{13}C spectroscopy. A SCARPER software package is available on request from the first author.

4. Summary

SCARPER offers significant bandwidth improvements for direct detection of X-spin spectra by the INEPT technique. It demonstrates comparable benefits for HSQC experiments, and should increase the accuracy of cross-peak intensities recorded in three-dimensional NOESY-HSQC spectra. It is not of course restricted to INEPT and HSQC; it should be useful for triple-resonance three- or four-dimensional experiments widely used in biomolecular NMR. For a given bandwidth, SCARPER reduces the radiofrequency power dissipation, a feature that is particularly important for cryogenic probes, and for fast-pulsing regimes where the relaxation delays are very short [35,36].

References

[1] M.H. Levitt, R. Freeman, NMR population inversion using a composite pulse, J. Magn. Reson. 33 (1979) 473–476.
[2] R. Freeman, S.P. Kempsell, M.H. Levitt, Radiofrequency pulses which compensate their own imperfections, J. Magn. Reson. 38 (1980) 453–479.
[3] T. Diercks, M. Daniels, R. Kaptein, Extended flip-back schemes for sensitivity enhancement in multidimensional HSQC-type out-and-back experiments, J. Biomol. NMR 33 (2005) 243–259.
[4] M.H. Levitt, R. Freeman, T. Frenkiel, Broadband heteronuclear decoupling, J. Magn. Reson. 47 (1982) 328–330.
[5] J.S. Waugh, Theory of broadband spin decoupling, J. Magn. Reson. 50 (1982) 30–49.
[6] A.J. Shaka, J. Keeler, T. Frenkiel, R. Freeman, An improved sequence for broadband decoupling: WALTZ-16, J. Magn. Reson. 52 (1983) 335–338.
[7] A.J. Shaka, P.B. Barker, R. Freeman, Computer-optimized decoupling scheme for wideband applications and low-level operation, J. Magn. Reson. 64 (1985) 547–552.
[8] T. Fujiwara, T. Anai, N. Kurihara, K. Nagawara, Frequency-switched composite pulses for decoupling carbon-13 spins over ultrabroad bandwidths, J. Magn. Reson. A 104 (1993) 103–105.
[9] J.-M. Böhlen, G. Bodenhausen, Experimental aspects of chirp NMR spectroscopy, J. Magn. Reson. A 102 (1993) 293–301.
[10] Z. Starcuk Jr., K. Bartusek, Z. Starcuk, Heteronuclear broadband spin-flip decoupling with adiabatic pulses, J. Magn. Reson. A 107 (1994) 24–31.
[11] M.R. Bendall, Broadband and narrowband spin decoupling using adiabatic spin flips, J. Magn. Reson. A 112 (1995) 126–129.
[12] E. Kupče, R. Freeman, Adiabatic pulses for wideband inversion and broadband decoupling, J. Magn. Reson. A 115 (1995) 273–276.
[13] E. Kupče, R. Freeman, Stretched adiabatic pulses for broadband spin inversion, J. Magn. Reson. A 117 (1995) 246–256.
[14] R. Fu, G. Bodenhausen, Ultra-broadband decoupling, J. Magn. Reson. A 117 (1995) 324–325.
[15] E. Kupče, R. Freeman, Optimized adiabatic pulses for wideband spin inversion, J. Magn. Reson. A 119 (1996) 145–149.
[16] E. Kupče, R. Freeman, An adaptable NMR broadband decoupling scheme, Chem. Phys. Lett. 250 (1996) 523–527.

[17] A. Tannus, M. Garwood, Improved performance of frequency-swept pulses using offset-independent adiabaticity, J. Magn. Reson. A 120 (1996) 264–268.
[18] A. Abragam, The Principles of Nuclear Magnetism, Clarendon Press, Oxford, 1961, p. 65.
[19] K. Stott, J. Stonehouse, J. Keeler, T.L. Hwang, A.J. Shaka, Excitation sculpting in high-resolution nuclear magnetic resonance spectroscopy: application to selective NOE experiments, J. Am. Chem. Soc. 117 (1995) 4199–4200.
[20] K. Ogura, H. Terasawa, F. Inagaki, Fully ^{13}C-refocused multidimensional ^{13}C-edited pulse schemes using broadband shaped inversion and refocusing pulses, J. Magn. Reson. B 112 (1996) 63–68.
[21] K. Ogura, H. Terasawa, F. Inagaki, An improved double-tuned and isotope-filtered pulse scheme based on pulsed field gradients and a wideband inversion shaped pulse, J. Biomol. NMR 8 (1996) 492–498.
[22] C. Zwahlen, S.J.F. Vincent, L.E. Kay, Analytical description of the effect of adiabatic pulses in IS, I_2S, and I_3S spin systems, J. Magn. Reson. 130 (1998) 169–175.
[23] P.C.M. van Zijl, T.L. Hwang, N.M. Johnson, M. Garwood, Optimized excitation and automation for high-resolution NMR using B_1-insensitive rotation pulses, J. Am. Chem. Soc. 118 (1996) 5510–5511.
[24] J. Iwahara, G.M. Clore, Sensitivity improvement for correlations involving arginine side-chain Nε/Hε resonances in multidimensional NMR experiments using broadband ^{15}N 180° pulses, J. Biomol. NMR 36 (2006) 251–257.
[25] C. Zwahlen, P. Legault, S.J.F. Vincent, J. Greenblatt, R. Konrat, L.E. Kay, Methods for measurement of intermolecular NOE's by multinuclear NMR spectroscopy: application to bacteriophage λ N-peptide/boxB RNA complex, J. Am. Chem. Soc. 119 (1997) 6711–6721.
[26] R.D. Boyer, R. Johnson, K. Krishnamurthy, Compensation of refocusing inefficiency with synchronized inversion sweep (CRISIS) in multiplicity-edited HSQC, J. Magn. Reson. 165 (2003) 253–259.
[27] T.L. Hwang, P.C.M. van Zijl, M. Garwood, Broadband adiabatic refocusing without phase distortion, J. Magn. Reson. 124 (1997) 250–254.
[28] M.H. Levitt, R. Freeman, Compensation for pulse imperfections in NMR spin-echo experiments, J. Magn. Reson. 43 (1981) 65–80.
[29] T.L. Hwang, A.J. Shaka, Water suppression that really works. Excitation sculpting using arbitrary waveforms and pulsed field gradients, J. Magn. Reson. A 112 (1995) 275–279.
[30] E. Kupče, R. Freeman, Compensation of spin coupling effects during adiabatic pulses, J. Magn. Reson. 127 (1997) 36–48.
[31] G.A. Morris, R. Freeman, Enhancement of nuclear magnetic resonance signals by polarization transfer, J. Am. Chem. Soc. 101 (1979) 760–762.
[32] G. Bodenhausen, D.J. Ruben, Natural abundance nitrogen-15 NMR by enhanced heteronuclear spectroscopy, Chem. Phys. Lett 69 (1980) 185–189.
[33] A.G. Palmer, J. Cavanagh, P.E. Wright, M. Rance, Sensitivity improvement in proton-detected two-dimensional heteronuclear correlation NMR spectroscopy, J. Magn. Reson. 93 (1991) 151–170.
[34] Possibly derived from the Italian *scappare* "escape" and reinforced in Cockney rhyming slang: *Scapa Flow*.
[35] P. Schanda, B. Brutscher, Very fast two-dimensional NMR spectroscopy for real-time investigation of dynamic events in proteins on the time scale of seconds, J. Am. Chem. Soc. 127 (2005) 8014–8015.
[36] E. Kupče, R. Freeman, Fast multidimensional NMR by polarization sharing, Magn. Reson. Chem. 45 (2007) 2–4.